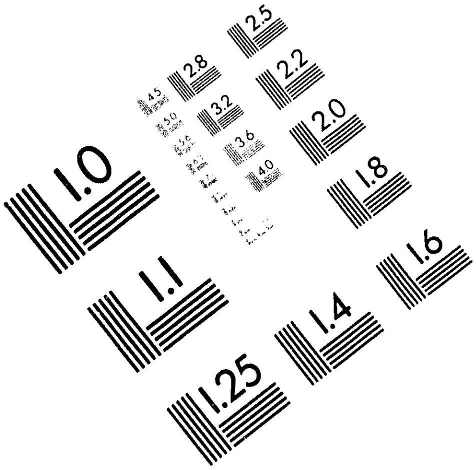

AIIM

Association for Information and Image Management

1100 Wayne Avenue, Suite 1100
Silver Spring, Maryland 20910
301/587-8202

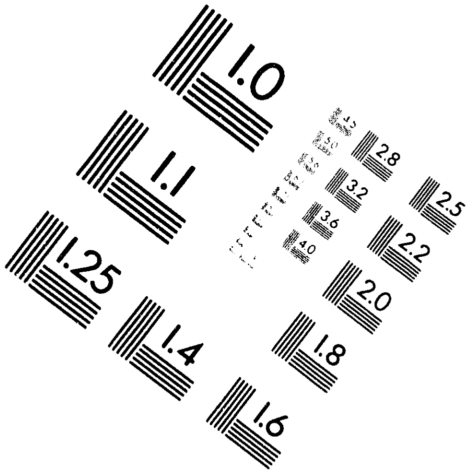

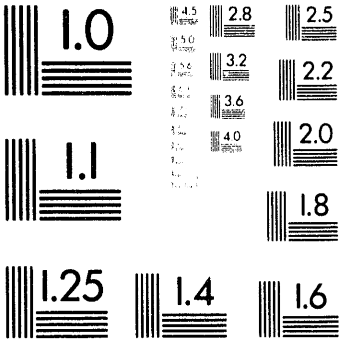

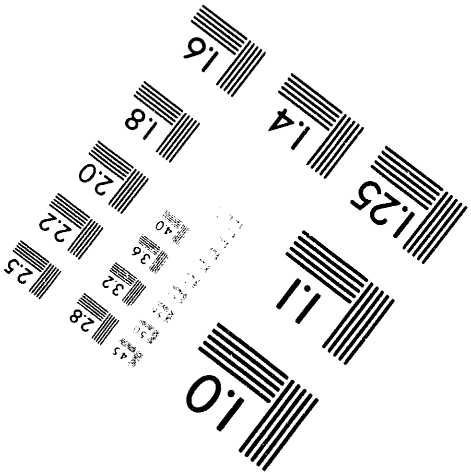

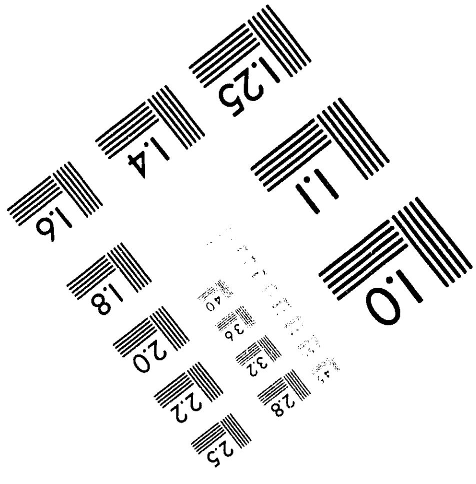

MANUFACTURED TO AIIM STANDARDS
BY APPLIED IMAGE, INC.

1 of 1

CONF-9406166--1 SAND94-0240C

NEW MATERIALS AND MULTIDIMENSIONAL CLUSTER ANALYSIS FOR SAW CHEMICAL SENSOR ARRAYS

Antonio J. Ricco, Gordon C. Osbourn, and John W. Bartholomew
Microsensor R&D and Vision Science Depts., Sandia National Laboratories
Albuquerque, New Mexico, USA 87185-0351

Richard M. Crooks and Chuanjing Xu
Department of Chemistry, Texas A&M University
College Station, Texas, USA 77843-3255

Ronald E. Allred
Adherent Technologies, Inc.
Albuquerque, New Mexico, USA 87123

ABSTRACT

We use six-element arrays of 97-MHz ST-quartz surface acoustic wave (SAW) devices to detect changes in thin-film mass and mechanical properties resulting from sorption of analytes by films representing two new classes of chemical sensor interface: self-assembled monolayers (SAMs) and plasma-grafted films (PGFs). While these materials do *not* display exceptional chemical selectivity, various combinations of the 7 different SAMs and 8 PGFs examined do produce distinct response patterns for each of 13 analytes. The analytes include aliphatic, aromatic, and chlorinated hydrocarbons; alcohols; ketones; organophosphonates; and water. Evaluation of the SAW array data using multidimensional cluster analysis techniques (**1**) shows that each chemical species can be correctly identified 100% of the time over the 9%- to 49%-of-saturation range using data from many combinations of four or more films.

INTRODUCTION

Chemical sensor arrays can obviate the difficult and costly process of developing a new thin film with high chemical specificity for each prospective analyte. Effective array technology hinges on two active research areas: new thin-film materials, and advanced mathematical techniques to identify the response patterns. In this paper, we describe the fabrication and application of two classes of thin-film materials, SAMs and PGFs, that we are evaluating for chemical sensing applications. Response data are reported for SAW devices coated with these materials during exposure over a range of concentrations to organic analytes representing several chemical classes.

For chemical sensor array data to be utilized efficiently, and also to guide the development and improvement of chemically sensitive films used with such arrays, requires effective pattern-recognition (PR) techniques. One promising technique for the analysis of chemical sensor array data has recently been adapted from multivariate cluster analysis software that mimics the way in which human beings group sets of objects together as a consequence of their spatial relationships to one another. This PR technique, developed by Sandia National Laboratories' Vision Science Dept., is described in detail in another paper in this Digest (**1**); only general results and trends obtained using the technique are reported here.

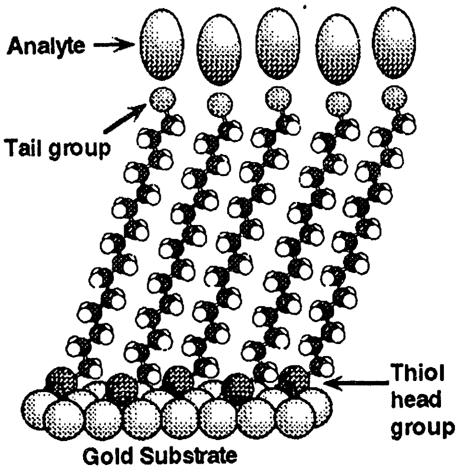

Figure 1. Schematic of interaction between self-assembled monolayer and analyte.

Self-assembled monolayers are ordered, molecular thin films (Figure 1) that can be prepared with a range of terminal groups to confer chemical preference for particular classes of analytes. The SAMs we have studied all include a thiol (-SH) head group separated by a seven- to 16-carbon chain from the terminal group. They are prepared on a gold film located between the launching and receiving sets of interdigital transducers (IDTs) on a SAW delay line surface. The two interactions responsible for the spontaneous assembly of these ordered films are (i) chemisorption of the thiol head group on the Au surface, and (ii) van der Waals forces between the long alkyl chains, maximized when the chains line up in the same relative orientation. As reported previously (**2**), combination of these materials with SAW devices allows monitoring of the kinetics of the monolayer assembly process, characterization of single-monolayer chemical reactions, and the construction of sensitive chemical detectors. Our current study includes SAMs with several terminal groups: methyl (CH_3); carboxylic acid (COOH); carboxylate-coordinated metal ions ($((COO^-)_2M^{2+}$, M = Fe, Ni, and Cu); cyano (CN); and amine (NH_2).

Plasma-grafted films are a little-studied class of polymeric materials with the potential to incorporate a wide range of functional groups in an open, permeable matrix (**3**). These films are formed (Figure 2) by plasma polymerization of a thin (one to several monolayers), highly crosslinked base layer that is sufficiently hydrogen-rich for a stable population of free radicals to persist after the plasma is extinguished. Following base layer formation, grafting occurs in the absence of plasma upon introduction of a suitably unsaturated

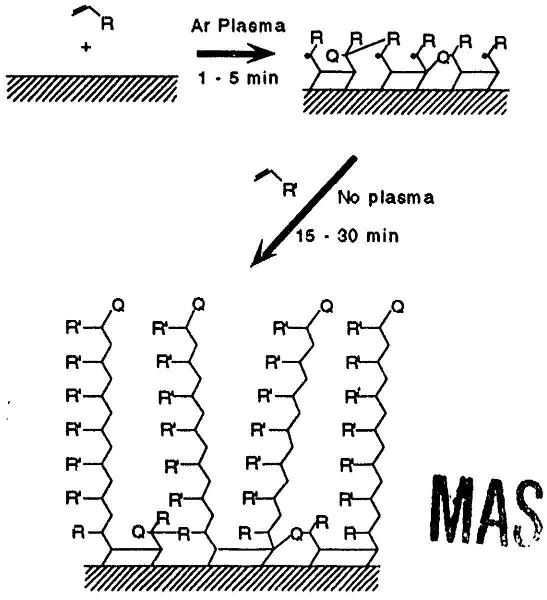

Figure 2. Formation of plasma-grafted film. Q is a free-radical quencher.

MASTER

DISTRIBUTION OF THIS DOCUMENT IS UNLIMITED monomer—e.g. one containing a vinyl functionality—in the gas phase. Residual free radicals on the base layer initiate a chain polymerization process; with appropriate monomers, polymerization is mainly straight-chain in nature, yielding the kelp-forest-like morphology shown in Figure 2. Grafting ceases when the gaseous monomer is removed and/or the radicals are quenched by O_2 or by recombination with one another. We have examined films derived from acrylic acid grafted onto a plasma-polymerized base layer of poly(isobutylene) or of acrylic acid itself. We have also investigated plasma-polymerized films of eugenol and vinylphosphonic acid.

The organic analytes studied include representatives of environmental pollutants, common industrial solvents, and chemical weapons simulants and precursors. Grouped according to general chemical class, they are cyclohexane and *i*-octane (aliphatic hydrocarbon); benzene and toluene (aromatic hydrocarbon); carbon tetrachloride and trichloroethylene (chlorinated hydrocarbon); methanol, *n*-propanol, and pinacolyl alcohol (alcohol); acetone (ketone); DIMP and DMMP (the organophosphonates diisopropylmethylphosphonate and dimethylmethylphosphonate, respectively); and water.

EXPERIMENTAL METHODS

SAW devices were designed and fabricated at Sandia National Laboratories (SNL) on ST-cut quartz substrates with propagation in the *X* direction. Devices have two interdigital transducers, each composed of fifty finger-pairs with $\Lambda = 32$ µm periodicity; v_o is 3.16 km/s, yielding a center frequency of 98 MHz. Transducers are defined photolithographically from 200 nm-thick Au on Cr; finger length is 50 Λ and center-to-center separation between transducers is 230 Λ . For SAM-coated devices, a 200 nm-thick layer of Au (with a Cr or Ti adhesion layer) was thermally or electron-beam deposited in the wave path using a shadow mask. Each SAW device was configured as the feedback element in an oscillator loop as described in detail elsewhere (4). This arrangement yields short-term frequency stability that allows the detection of mass changes of approximately 100 pg/cm^2 (4). The relationship between the frequency shift of a SAW delay-line oscillator circuit and the mass loading of the SAW is given by

$$\frac{\Delta f}{f_0} = \kappa \frac{\Delta v}{v_0} = -c_m f_0 \Delta(m/A), \qquad [1]$$

in which f_0 is the unperturbed oscillation frequency, v_0 is the unperturbed SAW velocity, κ is the fraction of the center-to-center distance between transducers perturbed, c_m is the coefficient of mass sensitivity (1.3 cm^2/g-MHz for ST-cut quartz), and $\Delta(m/A)$ is the change in mass/area. In addition to monitoring the SAW velocity using a frequency counter, we monitor the amplitudes of the input and output signals to/from the SAW device using a vector voltmeter, enabling the insertion loss (and hence SAW attenuation) to be measured (4). Each of the six oscillator loops used with the SAW array was connected in sequence to the frequency counter and vector voltmeter using a RF multiplexer (HP 3488A/44478A) that otherwise terminates the connections from each oscillator loop with 50 ohm loads.

Sets of six coated SAW devices were secured in a custom-fabricated test fixture utilizing spring-loaded pin contacts to the IDT bonding pads. Impedance matching consists of a single series inductor for one comb of each IDT; the other comb is grounded. With this configuration, total insertion loss of about 12 dB is attainable with the Cr/Au IDT SAW delay lines.

A manifold within the test fixture delivers the test gas stream to all six devices in parallel; a gas-tight O-ring seal encircles each SAW device. Vapor streams were provided by a computer-controlled gas-flow system, with the organic compound entrained by passing high-purity N_2 through a gas-washing bottle with a 50-mm diameter fritted disk; the vapor-saturated gas stream was diluted as required with additional N_2. Total flow rates were 1 l/min; the gas, organic liquid, and the SAW device were all maintained at 23° C.

Prior to deposition of the Au film and monolayer self assembly, SAW devices were silanized using $ClSi(CH_3)_3$ (Petrarch) to prevent interactions between polar compounds and the quartz substrate from complicating interpretation of the response. SAMs of mercaptoundecanoic acid (MUA, $HS(CH_2)_{10}COOH$; Aldrich) were produced by soaking Au-coated SAW devices in a dilute solution of the thiol in ethanol overnight. Amine and cyano-terminated monolayers were similarly prepared. Transition metals were coordinated to the MUA films by dipping for several minutes in a dilute ethanol solution of the perchlorate salt, then rinsing.

To form a plasma-polymerized acrylic acid base layer, a flask containing the monomer (Polysciences) was heated to 120 °C. A flow of 5 L/min of Ar entrained the compound, carrying it into a quartz plasma-deposition chamber, which was continuously pumped to maintain a pressure near 1 Torr (TC gauge). The 13.56-MHz plasma was maintained at a forward power of approximately 50 W. After plasma polymerization of the base layer (1 - 5 min), the RF generator was switched off and grafting of acrylic acid onto the base layer allowed to continue for 15 - 30 min at an indicated pressure of 1 Torr. Poly(isobutylene) base layers were produced using similar methods to the acrylic acid, except the monomer was obtained from a gas cylinder of isobutylene (Aldrich) at room temperature. Vinylphosphonic acid (Hoechst-Celanese) and eugenol (Polysciences) plasma-polymerized films were prepared analogously to the acrylic acid base layer, with the monomers held at approximately 80 °C in both cases.

RESULTS AND DISCUSSION

To obtain the maximum information from the coated SAW devices, both the velocity and the attenuation of the acoustic wave are continuously monitored (5). For each analyte, a four-hour adsorption/desorption isotherm was obtained, over the course of which the concentration of analyte slowly varied from 3% to 50% and back to 3% of its saturation vapor pressure, p_{sat}. For the isotherms shown below, note that data between 0% and 3% are not "real", because the flow system steps abruptly from 0 to 3%.

Figure 3 shows a set of four benzene adsorption isotherms obtained at approximately 30-day intervals using a single MUA-coated SAW device; frequency shift vs. partial saturation pressure is at the top, relative insertion loss vs. p/p_{sat} at the bottom. During the time periods between the isotherms of Figure 3, this coated device was exposed to the various other analytes in the test group, so the extent of reproducibility includes the effects of exposure to a range of chemicals. Variation of the isotherms from one measurement to the next is representative of the better films we have examined; many others behave nearly as well.

In Figure 3, the nonmonotonic nature of the frequency-shift isotherms and the peak in the relative-insertion-loss isotherms are both indicative of a non-mass-loading response, a result of either resonant energy transfer to the film or a relaxation process in the film. Such effects occur at particular concentrations of adsorbed analyte because mechanical film properties (sound velocity, relaxation times) are influenced by the quantity of adsorbate. Significantly, nonmonotonic isotherms such as those in Figure 3 *do not* pose any difficulty for our PR algorithms (**1**).

Figure 4 presents a series of isotherms representing four of the chemical classes we have studied: aromatic and chlorinated hydrocarbons, alcohols, and organophosphonates. For each compound, a set of six isotherms is presented for frequency shift vs. p/p_{sat}, and another set of six for relative insertion loss. For clarity, only the adsorption branches are shown in each case. Each of the six curves represents a different chemically sensitive film; the legends and the caption describe the films. Note that all twelve of the curves for a given analyte are obtained simultaneously using our array system; tens of concentration points are recorded for each film/analyte combination.

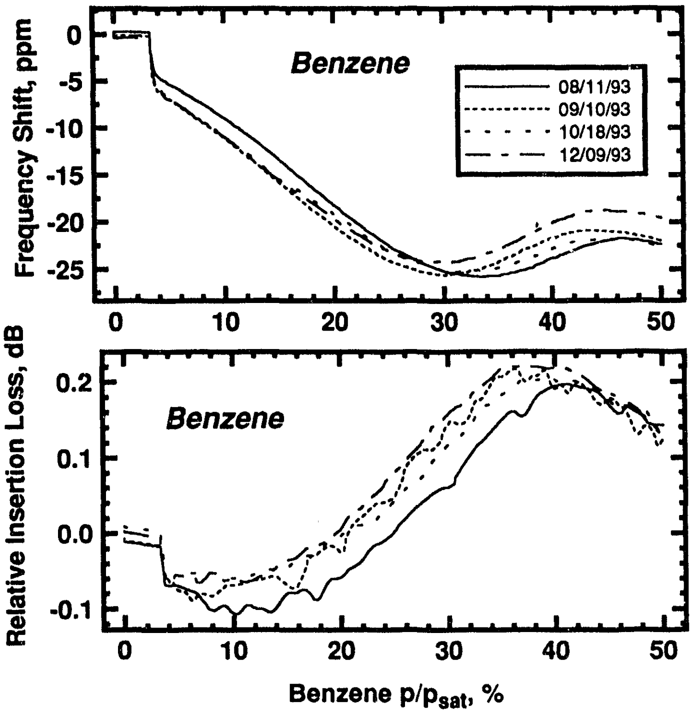

Figure 3. Benzene adsorption isotherms for a MUA self-assembled monolayer. Frequency data are in the top panel, corresponding insertion loss data at the bottom. The four isotherms were obtained on the dates in the legend; exposure to many other analytes occurred during the intervening time periods.

Examination of the six sets of six curves in Figure 4 reveals very significant qualitative differences in the pattern of responses for the four analytes. Each concentration of each analyte yields its own set of 12 responses; it is left as an exercise for the reader to show that each such set of 12 data points is unique.

The set of six films represented in Figure 4 gives flawless identification of each of the 13 analytes over the p/p_{sat} = 9% - 49% concentration using the "leave-one-out" approach with our PR technique (**1**). In this method, the data for each concentration of an analyte are represented by a k-dimensional vector, where k is the number of different responses collected. In the example shown by Figure 4, $k = 6$ because, at present, only the frequency-shift data for the six films are used. A cluster of all the (appropriately normalized (**1**)) data vectors but one is created for the analyte under consideration, and the full clusters are created for all other analytes. In the present example, 21 concentrations were used for each analyte (20 for the leave-one-out species). The concentration left out is then tested to see which cluster it groups with; for the example discussed here, the answer is invariably correct. Note that this sort of evaluation is rapid and straightforward with our PR technique, in contrast to some approaches—e.g., neural nets--in which complete "retraining" is required to evaluate each and every data point.

The relative insertion loss response provides useful information, both regarding the nature of the coating/analyte interaction, and for the purpose of correctly identifying the analyte. Note in particular the prominent peaks in the attenuation curves in three of the sets of isotherms, and the corresponding sigmoidal deflections in the frequency-shift data. As discussed above, this indicates a non-mass-loading response; it also serves as a signature for a particular analyte/film pair. Unfortunately, the higher noise level apparent in the relative insertion loss data makes use of this information more challenging. Nevertheless, we are working to include these data, which should allow use of a smaller number of films (array elements) to provide an equivalent level of certainty, thus reducing system cost, size, and complexity.

The six films represented in Figure 4 are equally divided among the two materials categories, SAMs and PGFs, a consequence of an evaluation using our PR system to find the best set(s) of films. This result supports our claim that chemical orthogonality of films is maximized when disparate film categories are included, and we therefore plan to broaden the film categories under examination to include metals, ceramics, coordination complexes, and others.

CONCLUSIONS

Combination of a SAW array with the appropriate chemically sensitive films and pattern-recognition algorithms provides a powerful method to monitor many different species without the need to custom design and synthesize a large number of custom thin films. The ability to handle often non-linear-with-concentration data produced by coated SAW devices is a strength of our multidimensional PR technique. We are currently exploring application of this combination of technologies for: detecting lower analyte concentrations; quantifying analytes; and analyzing simple chemical mixtures.

Helpful technical discussions with, and collaboration on the design of the six-device array fixture by, Stephen J. Martin of SNL are gratefully acknowledged, as is the excellent technical assistance of Alan W. Staton, Mary-Anne Mitchell, and Mark Hill, all of SNL, and Brent Gordon of Adherent Technologies. This work was supported by the U.S. DOE under contract DE-AC04-94AL85000.

REFERENCES

1. G. C. Osbourn, J. W. Bartholomew, G. C. Frye, and A. J. Ricco, "Clustering-Based Pattern Recognition Applied to Chemical Recognition Using SAW Array Signals", *Technical Digest of the 1994 Solid-State Sensor and Actuator Workshop*, Hilton Head Isl., SC, 6/13-16/94, Transducer Research Foundation, Cleveland (1994).

2. A. J. Ricco, L. J. Kepley, R. C. Thomas, L. Sun, and R. M. Crooks, "Self-Assembling Monolayers on SAW Devices for Selective Chemical Detection", *Technical Digest of the 1992 Solid-State Sensor and Actuator Workshop*, Hilton Head Island, SC, 6/21-25/92, IEEE, New York, pp. 114-117 (1992).

3. Y. L. Hsieh and M. Wu, "Residual Reactivity for Surface Grafting of Acrylic Acid on Argon Glow-Discharged Poly(Ethylene Terephthalate) (PET) Films", *J. Appl. Polymer Sci.*, *43*, 2067 (**1991**).

4. A. J. Ricco and S. J. Martin, "Thin Metal Film Characterization & Chemical Sensors: Monitoring Electronic Conductivity, Mass Loading, and Mechanical Properties with SAW Devices", *Thin Solid Films*, *206*, 94 (1992).

5. S. J. Martin and A. J. Ricco, "Effective Utilization of Acoustic Wave Sensor Responses: Simultaneous Measurement of Velocity and Attenuation", *Proc. 1989 IEEE Ultrasonics Symp.*, 621 (1989).

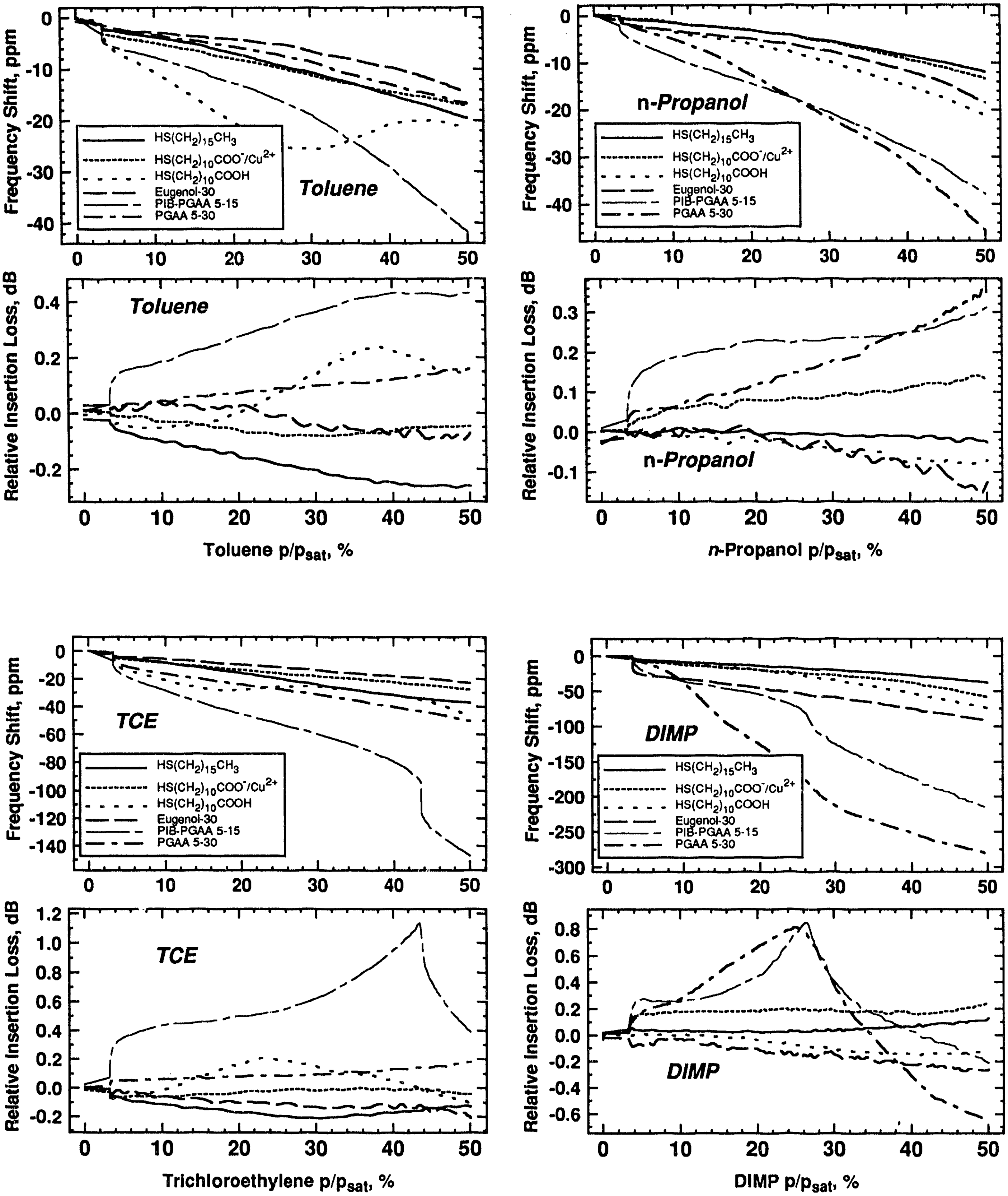

Figure 4. Six-SAW array adsorption isotherm sets for toluene (upper left), trichloroethylene (lower left), n*-propanol (upper right), and DIMP (lower right). Frequency shift data are above relative insertion loss data for each analyte. This set of six films (identified in the legends) gives 100%-accurate identification of these and 10 other analytes in conjunction with our pattern-recognition technique. The first three films in the legends are SAMs; eugenol-30 is a 30-min plasma-polymerized film of 2-methoxy-4-(2-propenyl)phenol; PIB-PGAA is a 5-min plasma-polymerized base layer of poly(isobutylene) + a 15-min graft of acrylic acid; and PGAA 5-30 is a 5-min base layer of plasma-polymerized acrylic acid + a 30-min graft of acrylic acid.*

DATE
FILMED

6/28/94

END